

NUMERICAL STUDY OF TUBE HYDROFORMING TECHNOLOGY

Viorel Paunoiu, Ovidiu Ciocan & Dumitru Nicoara

University “Dunarea de Jos” of Galati, Department of Manufacturing Science and Engineering Technology,
Domneasca Street, No. 111, 800201 Galati, Romania

Corresponding author: Viorel Paunoiu, viorel.paunoiu@ugal.ro

Abstract: The success in tube hydroforming (THF) technology depends on an appropriate loading path which could be described as the combination between the axial force or the axial punch displacement and the internal pressure. In the paper is presented a numerical study about the tube hydroforming process of a profiled part, considering as the main parameters the presence or the absence of the axial displacement of the punches and different friction coefficients. Using finite element method it has been demonstrated that the combination of the tube hydroforming process parameters could be determined very efficiently. The simulated results recommend the deformation with axial moving of the punches as the best method to control the part quality and to generate successful part without fracture or wrinkling failure.

Key words: hydroforming, bulge forming, simulation, FEM

1. INTRODUCTION

Tube hydroforming (THF) has been well-known since the 1950's. Tube hydroforming has been called by many other names such as bulge forming of tubes (BFT's), liquid bulge forming (LBF) and hydraulic (or hydrostatic) pressure forming (HPF) depending on the time and country in which it was used (Ahmetoglu, 2000). The stress state at a given time and location varies with the process history and the design and control of the load paths (Altan, 2005). Success of the tube hydroforming process depends on an appropriate combination of loading curve (internal pressure and axial feed at the tube ends), material properties and process conditions (Banabic, 2000). The process cycle for a typical tube hydroforming operation follows the sequence illustrated in figure 1 (Dohmann, 1996). First the tube (4) is placed between the dies (1, 4) (figure 1.a). Clamping device is used to close the dies and to apply sufficient clamping force. Tube (3) is filled with hydraulic fluid to provide necessary internal pressure. Axial punches (2) are used to provide initial sealing to avoid any pressure losses (figure 1.b). Fluid pressure within the tube is increased after the die closes to cause necessary deformation with simultaneous application of axial feeding to push the material into the

deformation zone (figure 1 c). The proper combination of axial feeding (F_{axial}) and internal pressure (p) are applied during the hydroforming process to improve hydroforming capabilities. The calibration phase starts once the tube touches the die. Axial feeding is not required during the calibration phase. Tube is subjected to large pressures to form corners radii. Finally, the bulged tube (5) is taken out of the die (figure 1. d).

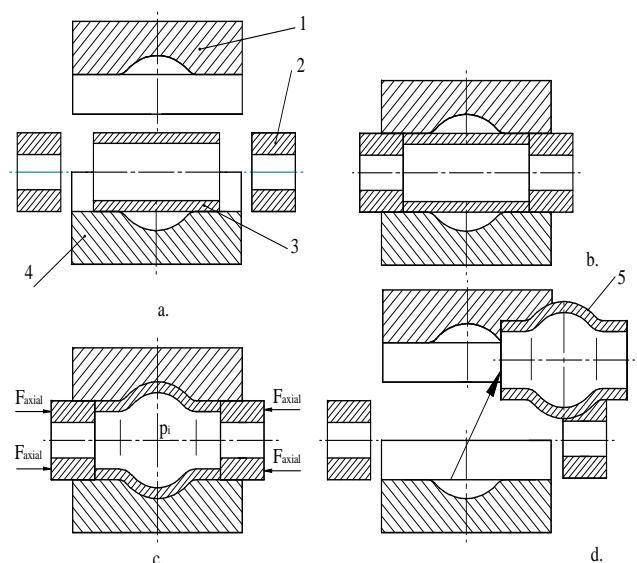


Fig. 1. Tube hydroforming process

Hydroformed tube parts have improved strength and stiffness, lower tooling cost, fewer secondary operations, and closed dimensional tolerances compared to stamping processes, thus an overall reduced manufacturing cost (Koç, 2008).

There are two ways to apply the axial compression, by controlling the axial force, or by controlling the axial punch displacement. Accordingly, the loading path can be described as the axial force or the axial punch displacement varies with the internal pressure (Yang, 2006).

The loading path of the hydraulic pressure and the axial pushing plays a significant role in the formability of the THF process (Hama, 2006). Some

methodologies had developed in this direction: the hydraulic pressure and the axial pushing are applied from the beginning of the process; hydraulic pressure is raised to a certain magnitude in advance of the axial pushing and then the hydraulic pressure and the axial pushing are simultaneously applied.

As it follows it will present some comparative results about the tube hydroforming process simulation of a symmetrical part, considering as the main parameter the presence or the absence of the axial displacement of the punches. In this study the presence of the axial displacement and the pressure are applied from the beginning.

2. TUBE HYDROFORMING PROCESS SIMULATION

Finite Element Analysis (FEA) is a powerful simulation tool for analyzing complex three dimensional sheet metal forming problems during the die design stage or as a troubleshooting tool in the production mode (Paunoiu, 2007). Finite element method (FEM) simulation of the hydroforming process has been proven to be an advantageous tool in assisting quality designs. The most straightforward approach is to use an FEM model with a predetermined set of control parameters and evaluate the process simulation with respect to process parameters/loading paths (i.e. internal pressure and axial feed), part geometry, and part formability by analyzing the thinning, thickening, and strain distribution in the deformed tube (Jirathearanat, 2004). The processes of circular bulging and T-shape formation were simulated by Aue-u-lan (2005), Hama (2006), Batalha (2005) and Chenot (2006) using different FEM codes.

The commercial DYNIFORM-PC solution package was developed to study the issues stated above and to assist the die designer and stamping engineer in meeting rapid prototyping requirements.

For tube hydroforming simulation two cases were analysed: the deformation without axial moving of the punches and the deformation with axial moving of the punches, considering as the part, the one presented in figure 2.

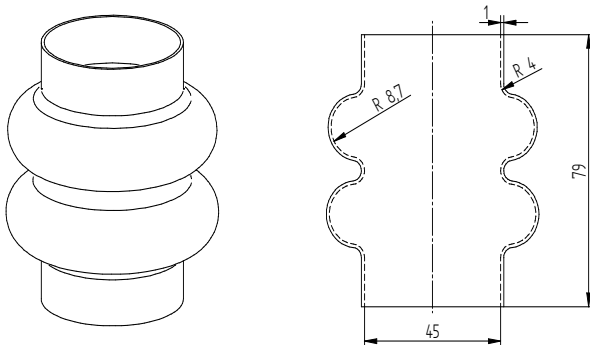


Fig. 2. Part considered for obtaining using tube hydroforming process

The general FEM model of the tools for deformation is presented in figure 3.

The difference, between the two models is the presence of the two plates at the ends of the tub in the case of the deformation with axial moving of the punches.

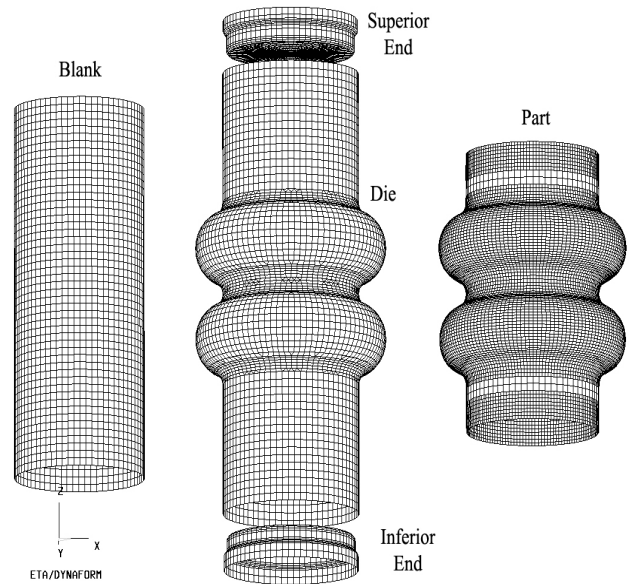


Fig. 3. Simulation model in tube hydroforming process

These plates simulate the hydraulic ends of the axial pistons, which are in contact with the tube and are moving axially. The die and the two ends were defined as rigid bodies.

The blank is a tube ($\Phi 45 \times 100 \times 1$ mm).

For the tube material, the true stress – logarithmic plastic strain is approximated by the Power law:

$$\sigma = K \cdot \epsilon^n \quad (1)$$

where: K is the constant of the material, $K = 546.9$ MPa; n – strain hardening coefficient, $n = 0.19$. The material is characterized by the following anisotropy coefficients $r_{00} = 1.65$; $r_{45} = 1.25$; $r_{90} = 1.80$.

Four-node Belytschko-Tsay shell elements with 5 integration points on the thickness were employed for the tube in the simulation due to its computational efficiency and accuracy.

The interface between the tube and the die was modeled with an advanced automatic surface-to-surface contact algorithm with an elastic coulomb friction law. Three friction coefficients were considered: 0.125; 0.1; 0.05.

The number of finite elements used was of 6772 for the die; 3400 for the blank and 1830 for the two ends. According to Koç (2008) the maximum pressure necessary to deform the tube (considering only a single bulge), without fracture, could be evaluated using the relation:

$$p = 2 R_m \frac{g_i}{D_i - g_i} \quad (2)$$

where:

- R_m is the ultimate tensile strength, $R_m=398.9$ MPa;
 - g_i – initial thickness of the tube, $g_i=1$ mm;
 - D is the diameter of the die cavity, $D_i = 47$ mm.
- Using the values of the above parameters it results equal with 17.7 MPa.

Starting from this value we simulate the process, and it results that for obtaining the two bulges of the part is necessary a pressure of 35 MPa.

The loading pressure used, in both deformation cases was limited at 35 MPa for a total computational time of 0.04 s, and the variation of it in time is presented in figure 4.

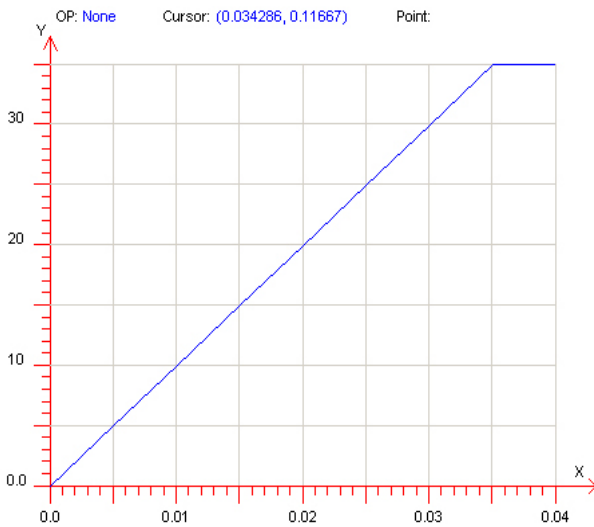


Fig. 4. Pressure-time variation for deformation

In the second case were defined the axial displacements of the two ends. It's were chooses equal with 10.5 mm for both ends.

Some results of the numerical simulations are presented in what it follows.

3. RESULTS AND DISCUSSIONS

The state of strain and stress is determined for the three different zones of the tube expansion: linear (guiding) (1) transition (2) and free expansion (3) zones (figure 5).

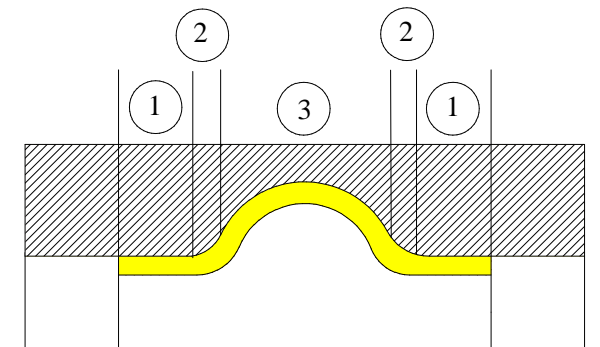


Fig. 5. Charactersitic zones in hydroforming

The parts obtained by simulation were measured point to point along the axial direction starting from the linear zone to expansion zone according to figure 4. In the below figures these points are named arbitrary points.

The deformation stages are presented in figure 6. It could be made next observations:

a. Thickness:

In the first case, the tubular element is allowed to expand freely. The tube wall will thin and the radius will increase in the expansion zone (figure 7).

We observe that the tube is thinner in the maximum expansion zone (less than 0.8 mm in comparison with the initial value of 1 mm). For a coefficient of friction of 0.1, the value of maximum thinning is 21.02 % according to the simulation and appears in the above specified zone.

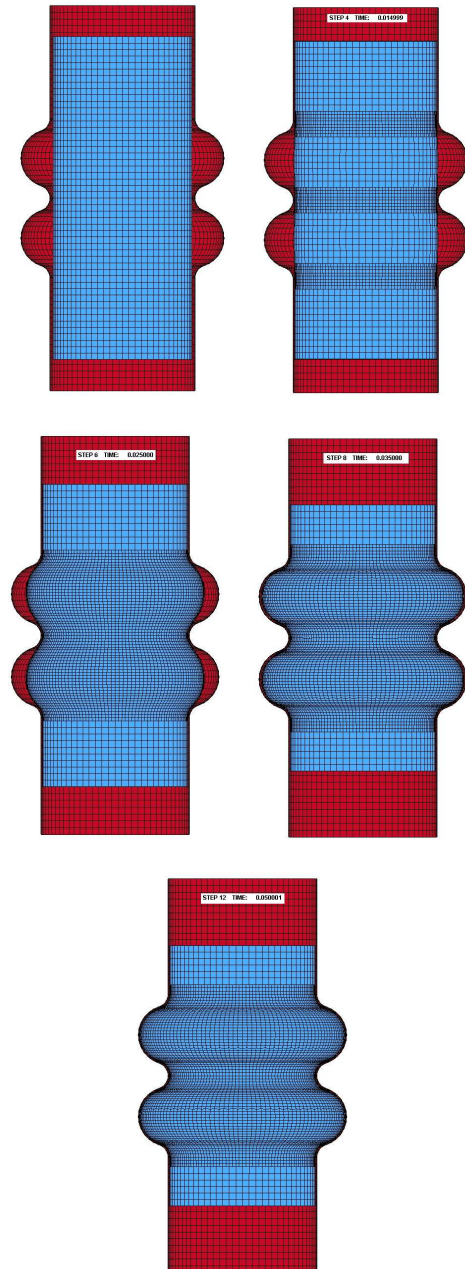


Fig. 6. Deformation stages in tube hydroforming

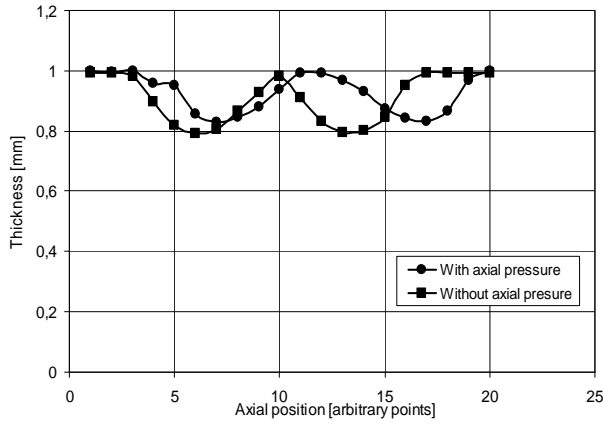


Fig. 7. Thickness variations in tube hydroforming process (friction coefficient of 0.1)

In the second case, the thickness variation is more constant in the expansion zone, because axial displacement of the two ends produced a supplementary compression of the tube frontends which affects the material behaviour under pressure. The value of maximum thinning is 17.84% according to the simulation and appears in the above specified zone. Material thickening in the tube ends is about 0.81% because of the axial moving. Similar variations are obtaining using the others two values of friction coefficients.

The values of thinning are presented in table 1.

Table 1. Part thinning variation, [%]

Friction coefficient	Without axial moving			With axial moving		
	0.125	0.1	0.05	0.125	0.1	0.05
Thinning, [%]	21.94	21.02	20.58	14.69	17.84	17.68

It can be seen from the above table, with decreasing the value of friction coefficient in the case of deformation without axial moving of the punches, the material thinning are also decreasing as a result of the material flow improving. In the second case, the decreasing of the friction coefficient it seems to not affect the value of thinning in the conditions of normal and high lubrication.

b. Plastic Strain:

The plastic strain can be calculated based on Von Mises criterion as follows:

$$\bar{\epsilon} = \sqrt{\frac{2}{3}(d\epsilon_1^2 + d\epsilon_2^2 + d\epsilon_3^2)} \quad (3)$$

where $d\epsilon_1$, $d\epsilon_2$, $d\epsilon_3$ are the hoop (tangential or circumferential), thickness (radial) and longitudinal (axial) principal strains.

In the first case, the plastic strain in the guiding zone is negligible (figure 7) and it becomes maximum in the expanding zones.

In the second case the plastic strain in the guiding zone is also negligible (see also figure 8) and become

maximum in expansion zone. Also in this case, in the front edges of the tube the plastic strain has higher value because of axial moving. Both curves are similar with the die profile.

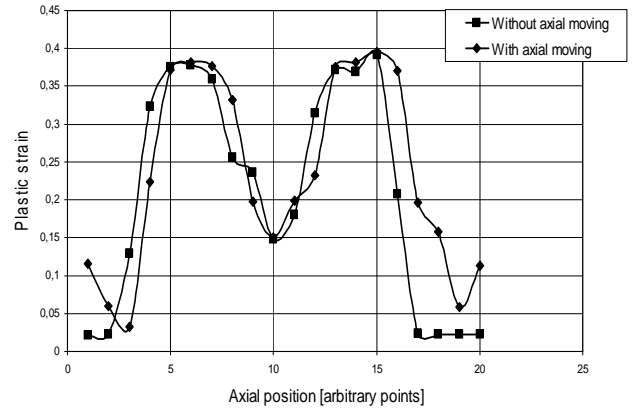


Fig. 8. Plastic strain variations in tube hydroforming process (friction coefficient of 0.1)

Similar variations are obtaining using the others two values of friction coefficients.

c. Sliding velocity:

We characterize this process measure using the total velocity parameter. In the first case of deformation the variation of the total velocity is non uniform and is bigger in the expansion zones. In the second case the total velocity is also non uniform. There are big differences between the values of the total velocities in the two cases at the tube edges, as it results from figure 9.

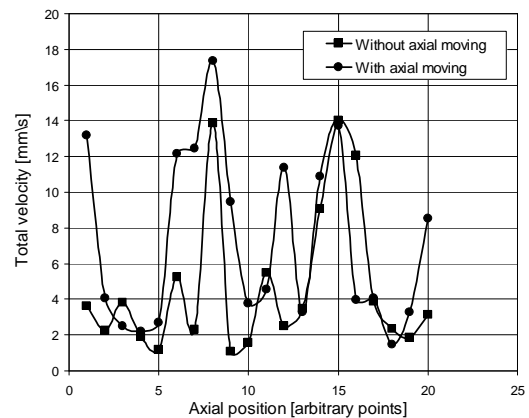


Fig. 9. Total velocity variations in tube hydroforming process (friction coefficient of 0.1)

In the case of deformation without axial displacement, the values of the velocities have almost a similar variation as the die profile and are mainly influenced by the friction, firstly are smaller in the linear zone, then are increasing starting with transition zone, become maximum in the expansion zone, decreasing in the transition zone, become smaller in the linear zone and so on. In the case of deformation with axial displacement, the values of the velocities in the linear zones decreasing as a

result of the imposed axial moving and friction. Similar variations are obtaining using the others two values of friction coefficients.

d. Forming Limit Diagram

The forming limit diagram (FLD) is a tool used to allow a correct analysis of the material formability. The vertical axis represents the percentage of major strain and the horizontal axis represents the percentage of minor strain. The strain state of a part can be represented on the FLD by plotting its major and minor strains.

Major strain in most tube hydroforming processes is in the circumferential direction, as expansion in the radial direction is dominant as compared with elongation in the axial direction.

As it results from the figures 10-11, most of the data points appeared in the region of negative minor strain on the FLD. There exist numerous data points in the area beyond the uniaxial tension mode as the reduction in the thickness decreases due to the axial feed of the material.

In the case of hydroforming without axial feeding (figure 10), a tendency of crack appearance in the regions of the material expansions is present.

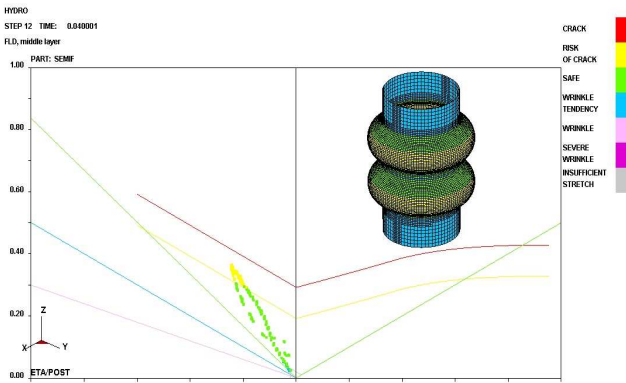


Fig. 10. FLD for deformation without axial punches moving (friction coefficient of 0.1)

In the case of hydroforming with axial feeding (figure 11) the crack appearance is avoid as a result of supplementary moving of the material during the deformation.

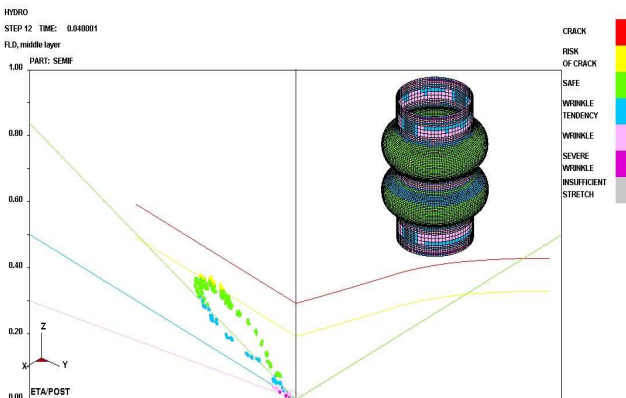


Fig. 11. FLD for deformation with axial punches movings (friction coefficient of 0.1)

e. Von Misses:

The effective stress is calculated using Von Mises criterion:

$$\bar{\sigma} = \frac{1}{\sqrt{2}} \sqrt{(\sigma_1 - \sigma_2)^2 + (\sigma_2 - \sigma_3)^2 + (\sigma_1 - \sigma_3)^2} \quad (4)$$

where $\sigma_1, \sigma_2, \sigma_3$ are the hoop (tangential or circumferential), thickness (radial) and longitudinal (axial) principal stress.

In the first case, the values of the maximum Von Mises stress (figure 12) show that the entire piece supports a plastic deformation. The value of this stresses no exceed the fracture limit. The upper value of 505.74 MPa is not bigger than the admisible breaking value of the material that is 700 MPa.

In the second case of deformation, the upper value of 497.97 MPa Von Mises stresses is not bigger than the admisible breaking value of the material that is 700 MPa.

The variation of this parameter is presented in table 2.

Table 2. Von Mises variation

Friction coefficient	Without axial moving			With axial moving		
	0.125	0.1	0.05	0.125	0.1	0.05
Von Mises	504.7	505.7	507.3	482.1	497.9	504.9

The decreasing of friction coefficient improves the material deformation having as a result the increasing of the Von Mises stresses values (table 2).

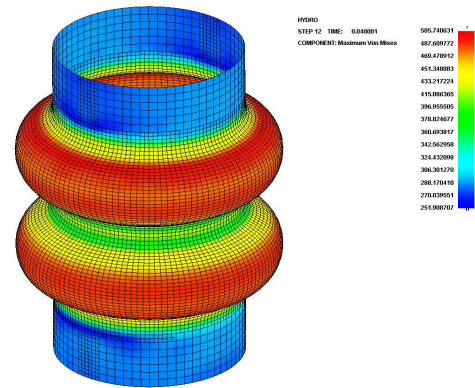


Fig. 12. Von Mises stresses for deformation without axial punches movings (friction coefficient of 0.1)

f. Friction coefficient:

The friction coefficient has an important role both in simulation and in the real case of deformation. The numerical results in connection with the part height are presented in table 3, for the two cases of deformation.

Table 3. Part height variation

Friction coefficient	Without axial moving			With axial moving		
	0.125	0.1	0.05	0.125	0.1	0.05
Part height	80.91	79.711	77.684	80.44	77.39	75.65

It can be seen from the above tabel, with decreasing the value of friction coefficient, the part height are also decreasing as a result of the material flow improving.

4. CONCLUSIONS

Using finite element analysis methods it has been demonstrated that hydroforming process parameters can be determined very efficiently. Simulation of tube hydroforming process with profilated die were carried out considering the presence or the absence of the axial compression and different friction coefficients.

In the case of the deformation with axial compression the thickness variation is more uniform having as a result a better quality of the part.

In the case of the deformation with axial compression, a supplementary deformation appears at the ends of the part, which will imply an addition operation of cutting.

The friction conditions limit the material flow in the die. As a result the friction coefficient influences the dimension of the part and also the material thinning. The level of stresses is bigger when the friction coefficient is bigger and also in the case of the deformation with axial compression. So, decreasing the friction will result in an increase in the formability of tubes.

The presence of axial compression could be used to control the part height and the level of this is dependent of the friction coefficient.

For industrial point of view the obtained results recommend the deformation with axial moving of the punches as the best method of manufacturing.

5. FUTURE RESULTS

Based on the above results, there are almost three directions of research in the near future:

- The first one is the establishment of the correlation between the simulations and experiments;
- The second one will be a more deeply study of the effect of friction toward the process quality;
- The third one will include the optimisation of the procees parameters for obtaining a more realistic dependence between the inside pressure and the axial movings of the punches;

6. REFERENCES

1. Ahmetoglu M.; Altan T. (2000), *Tube hydroforming: state-of-the-art and future trends*, Journal of Materials Processing Technology, Vol. 98, pp. 25-33, ISSN: 0924-0136.
2. Altan T. et al. (2005), *Virtual Process Development in Tube Hydroforming*, Journal of Materials Processing Technology, Vol. 146, Issue 1, pp. 130-136, ISSN: 0924-0136
3. Aue-u-lan, Y.; Ngaile, G., and Altan, T. (2005), *Optimizing Tube Hydroforming using Process*

Simulation and Experimental Verification, Journal of Materials Processing Technology, Vol. 146, Issue 1, pp. 137-143, ISSN: 0924-0136

4. Banabic D.; Bunge H.-J., Pöhlandt K., Tekkaya A.E. (2000), *Formability of Metallic Materials: Plastic Anisotropy, Formability Testing, Forming Limits*, Springer, ISBN 3-540-67906-5
5. Batalha, G.F. (2005), *Experimental and Numerical Simulation of Tube HydroForming*. Journal of Materials Processing Technology, Vol. 164-165, pp. 1140-1147., ISSN: 0924-0136
6. Chenot, J.L.; Masoni, L. (2006), *Finite element modelling and control of new metal forming processes*, International Journal of Machine Tools & Manufacture 46, pp.1194–1200, ISSN 0890-6955
7. Dohmann, F.; Hartl, Ch. (1996), *Entwicklungen und Anwendungen des Innenhochdruckumformens*, Blech Rohre Profile 43, pp. 30-35
8. Habraken, A. M. (2001), *Material forming processes*, Hermes Science Publications, Paris, ISBN 1-903996-33-3
9. Hama, T.; Ohkubo, T.,Kurusu, K.,Fujimoto, H., Takuda, H. (2006), *Formability of tube hydroforming under various loading paths*, Journal of Materials Processing Technology 177, pp. 676–679, ISSN: 0924-0136
10. Jirathearanat S.; et al (2004), *Tube Hydroforming of Y-shapes-Product and Process Design Using FEA Simulations and Experiments*, Journal of Materials Processing Technology, Vol. 146, pp. 124-129, ISSN: 0924-0136
11. Koç, M. (2008), *Hydroforming for advanced manufacturing*, Woodhead Publishing Ltd., ISBN 9781845693282
12. Massoni, E. (2001), *Finite element simulation of tube hydroforming process*, Proceedings of the Fourth International ESAFORM Conference on Materials Forming, pp. 381–384, 23–25 April, Liege, Belgium
13. Paunoiu, V.; Nicoara D., Ciocan, O. (2003), *Design of an experimental device for tube hydroforming technology*, The Annals of Dunarea de Jos University of Galati, Fascicle V, Technologies in Machine Building, pp. 47-52, ISSN 122-4566
14. Paunoiu, V; Nicoara, D., Ciocan, O., Ghita, E. (2007), *Simulation of reconfigurable tube hydroforming technology*, The Annals of Dunarea de Jos University of Galati, Fascicle V, Technologies in Machine Building, pp. 99-103, ISSN: 1221-4566
15. Siegert, K.; Häussermann M., Losch B., Rieger R. (2000), *Recent developments in hydroforming technology*, Journal of Materials Processing Technology, Vol. 98, pp. 251-258, ISSN: 0924-0136.
16. Yang, B.; Zhang, W.G., Li, S.H. (2006), *Analysis and finite element simulation of the tube bulge hydroforming process*, International Journal Advanced Manufacturing Technology, 29, pp. 453-458

Received: 23 January 2010 / Accepted: 10 May 2010 / Abstract published online: 18 May 2010

© International Journal of Modern Manufacturing Technologies